12. Matsuoka, S., Huang, M. & Elledge, S. J. Linkage of ATM to cell cycle regulation by the Chk2 protein kinase. *Science* **282,** 1893–1897 (1998).
13. Bell, D. W. *et al.* Heterozygous germ line hCHK2 mutations in Li–Fraumeni syndrome. *Science* **286,** 2528–2531 (1999).
14. Gu, Y., Rosenblatt J. & Morgan, D. O. Cell cycle regulation of CDK2 activity by phosphorylation of Thr160 and Tyr15. *EMBO J.* **11,** 3995–4005 (1992).
15. Boddy, M. N., Furnari, B., Mondesert, O. & Russell, P. Replication checkpoint enforced by kinases Cds1 and Chk1. *Science* **280,** 909–912 (1998).
16. Furnari, B., Rhind, N. & Russell, P. Cdc25 mitotic inducer targeted by chk1 DNA damage checkpoint kinase. *Science* **277,** 1495–1497 (1997).
17. Peng, C. Y. *et al.* Mitotic and G2 checkpoint control: regulation of 14-3-3 protein binding by phosphorylation of Cdc25C on serine-216. *Science* **277,** 1501–1505 (1997).
18. Sanchez, Y. *et al.* Conservation of the Chk1 checkpoint pathway in mammals: linkage of DNA damage to Cdk regulation through Cdc25. *Science* **277,** 1497–1501 (1997).
19. Zeng, Y. *et al.* Replication checkpoint requires phosphorylation of the phosphatase Cdc25 by Cds1 or Chk1. *Nature* **395,** 507–510 (1998).
20. Chehab, N. H., Malikzay, A., Appel, M. & Halazonetis, T. D. Chk2/hCds1 functions as a DNA damage checkpoint in G_1 by stabilizing p53. *Genes Dev.* **14,** 278–288 (2000).
21. Sun, Z., Hsiao, J., Fay, D. S. & Stern, D. F. Rad 53 FHA domain associated with phosphorylated Rad9 in the DNA damage checkpoint. *Science* **281,** 272–274 (1998).
22. Durocher, D., Henckel, J., Fersht, A. R. & Jackson, S. P. The FHA domain is a modular phosphopeptide recognition motif. *Mol. Cell* **4,** 387–394 (1999).
23. Hirao, A. *et al.* DNA damage-induced activation of p53 by the checkpoint kinase Chk2. *Science* **287,** 1824–1827 (2000).
24. Chan, T. A., Hermeking, H., Lengauer, C., Kinzler, K. W. & Vogelstein, B. 14-3-3σ is required to prevent mitotic catastrophe after DNA damage. *Nature* **401,** 616–620 (1999).
25. Giaccia, A. J. & Kastan, M. B. The complexity of p53 modulation: emerging patterns from divergent signals. *Genes Dev.* **12,** 2973–2983 (1998).
26. Lim, D. S. *et al.* ATM phosphorylates p95/nbs1 in an S-phase checkpoint pathway. *Nature* **404,** 613–617 (2000).
27. Xie, G. *et al.* Requirements for p53 and ATM gene product in the regulation of G1/S and S phase checkpoints. *Oncogene* **16,** 721–736 (1998).
28. Galaktionov, K. *et al.* CDC25 phosphatases as potential human oncogenes. *Science* **269,** 1575–1577 (1995).
29. Lee, J. S., Collins, K. M., Brown, A. L., Lee, C. H. & Chung, J. H. hCds1-mediated phosphorylation of BRCA1 regulates the DNA damage response. *Nature* **404,** 201–204 (2000).
30. Santoni-Rugiu, E., Falck, J., Mailand, N., Bartek, J & Lukas, J. Involvement of Myc activity in a G1/S-promoting mechanism parallel to the pRb/E2F pathway. *Mol. Cell. Biol.* **20,** 3497–3509 (2000).

Acknowledgements

We thank S. Elledge, G. Evan, S. I. Reed and Y. Shiloh for providing reagents; K. Hansen for advice; and the Danish Cancer Society, the Human Frontier Science Programme, Alfred Benzon's Fund, the European Commission, the Danish Medical Research Council and the Danish Cancer Research Fund for financial support.

Correspondence and requests for materials should be addressed to J.B. (e-mail: bartek@biobase.dk).

correction

arrow encodes an LDL-receptor-related protein essential for Wingless signalling

Marcel Wehrli, Scott T. Dougan, Kim Caldwell, Louise O'Keefe, Stephanie Schwartz, Dalit Vaizel-Ohayon, Eyal Schejter, Andrew Tomlinson & Stephen DiNardo

Nature **407,** 527–530 (2000).

This paper contained a mistake in Fig. 4a–d. The correct data are described below and are shown on our web site (http://www.med.upenn.edu/~cellbio/arrow.html). The main conclusions remain unchanged. In the paper, we used a LacZ enhancer trap inserted at *Distal-less* to investigate its regulation by *arrow*. However, as both *Distal-less* and *arrow* are on chromosome 2R, the LacZ reporter was flipped away in making *arrow* mutant clones. We have repeated these experiments using anti-Distal-less antibodies generating marked, *Minute+ arrow*^{2} mutant clones. Early-induced *arrow* mutant clones do not survive well; those that do survive exhibit loss of Distal-less expression. Later-induced clones show reduced Distal-less, although there is still residual expression. It is possible that the residual expression is due to perdurance of Arrow protein in cells only recently made mutant for *arrow*. As we stated in the paper, these results with *arrow* are quite similar to those obtained for clones mutant for *frizzled frizzled2* (C. M. Chen and G. Struhl, *Development* **126,** 5441–5452; 1999). In the legend to Fig. 4, however, we noted the higher level of Distal-less expression in the wild-type twin spots compared to the heterozygous tissue. Rather than reflecting changes in Wnt signalling, this resulted simply from the presence of two copies of the Distal-less LacZ reporter on the wild-type twin spots. □

erratum

Polo-like kinase 1 phosphorylates cyclin B1 and targets it to the nucleus during prophase

Fumiko Toyoshima-Morimoti, Eri Taniguchi, Nobuko Shinya, Akihiro Iwamatsu & Eisuke Nishida

Nature **410,** 215–220 (2001).

Figure 5g was printed in black and white instead of in colour. The Figure is reproduced in colour below. □

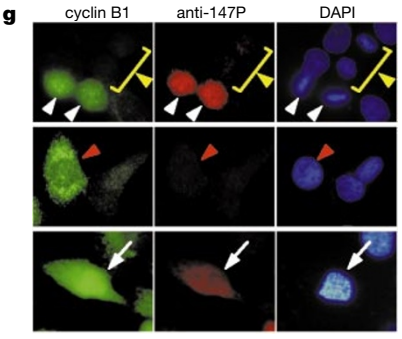

arrow encodes an LDL-receptor-related protein essential for Wingless signalling

Marcel Wehrli*†‡, Scott T. Dougan‡§, Kim Caldwell§, Louise O'Keefe§, Stephanie Schwartz*§, Dalit Vaizel-Ohayon‖, Eyal Schejter‖, Andrew Tomlinson† & Stephen DiNardo*§

** University of Pennsylvania School of Medicine, BRB II Room 1223, 421 Curie Boulevard, Philadelphia, Pennsylvania 19104, USA*
† Columbia University, 710 West 168th Street, New York, New York 10032, USA
§ Rockefeller University, 1230 York Avenue, New York. New York, 10021, USA
‖ Weizmann Institute of Science, Rehovot 76100, Israel
‡ These authors contributed equally to this work

The Wnt family of secreted molecules functions in cell-fate determination and morphogenesis during development in both vertebrates and invertebrates (reviewed in ref. 1). *Drosophila* Wingless is a founding member of this family, and many components of its signal transduction cascade have been identified, including the Frizzled class of receptor. But the mechanism by which the Wingless signal is received and transduced across the membrane is not completely understood. Here we describe a gene that is necessary for all Wingless signalling events in *Drosophila*. We show that *arrow* gene function is essential in cells receiving Wingless input and that it acts upstream of Dishevelled. *arrow* encodes a single-pass transmembrane protein, indicating that it may be part of a receptor complex with Frizzled class proteins. Arrow is a low-density lipoprotein (LDL)-receptor-related protein (LRP), strikingly homologous to murine and human LRP5 and LRP6. Thus, our data suggests a new and conserved function for this LRP subfamily in Wingless/Wnt signal reception.

In each embryonic segment, Wingless (Wg) is expressed anterior to cells expressing Engrailed (En) which co-express the signal Hedgehog (Hh). Most of the pattern across each segmental field is organized by these two signals. For example, Wg has two roles in patterning the segment. First, between 3 and 6 hours after egg laying (a.e.l.), early Wg signalling is necessary for the continued expression of En and Hh in the adjacent cell row. This ensures the maintenance of the parasegmental subdivisions of the body axis, generating the segmental body plan observed in larval cuticle preparations (Fig. 1a). Between 6 and 9 hours a.e.l., Wg signalling assigns specific cell fates. Within each segment, ventral epidermal cells secrete either smooth cuticle or protrusions called denticles. The double row of En/Hh-expressing cells straddles the boundary between smooth cuticle and the first denticle row (Fig. 1b). Wg signalling instructs anterior En cells to adopt smooth cell fate[2]. When Wg function is eliminated after 8 hours a.e.l., the anterior En cell incorrectly adopts a denticle fate (Fig. 1c). Similarly, anterior En cells adopt denticle fates in *arrow* mutants (Fig. 1d). These embryos have wild-type segmentation because early Wg signalling proceeds normally in zygotic *arrow* mutants. However, when we removed both maternal and zygotic *arrow* function (Fig. 1e; hereafter referred to as arr^{null} embryos), the resulting embryos were indistinguishable from *wg* null mutants. As the maintenance of En expression depends on the reception of the early Wg signal, we assayed arr^{null} embryos for En maintenance. En expression is initiated properly in *wg* and arr^{null} embryos (Fig. 1f, h, j) but then fades (Fig. 1g, i, k). In addition, Wg protein is distributed normally in arr^{null}mutant embryos, as compared with wild-type embryos (Fig. 1l; and data not shown). In particular, in arr^{null} embryos Wg is still detectable within cells distant from the Wg-expressing cells. Thus, *arr* mutations do not affect the production of ligand, nor its distribution across the epithelium, but nevertheless block the two Wg-dependent patterning events in embryonic epidermis. Furthermore, *arrow* function is required for all other Wg signalling events that we have tested, such as in embryonic midgut (data not shown), as well as in all facets of imaginal disk patterning (see below). Thus, *arrow* conforms to the expectation for a gene encoding an essential component of the Wg pathway.

We cloned the *arrow* gene using a lethal P-element insertion (l(2)k08131) that fails to complement *arrow*. The longest complementary DNA (6,012 base pairs (bp); GenBank AY005815, CT15575) restores smooth cuticle to alternate segments of arr^{null} embryos when expressed under control of Prd–GAL4, indicating rescue of Arrow function and Wg signalling (Fig. 2a, compare with Fig. 1e).

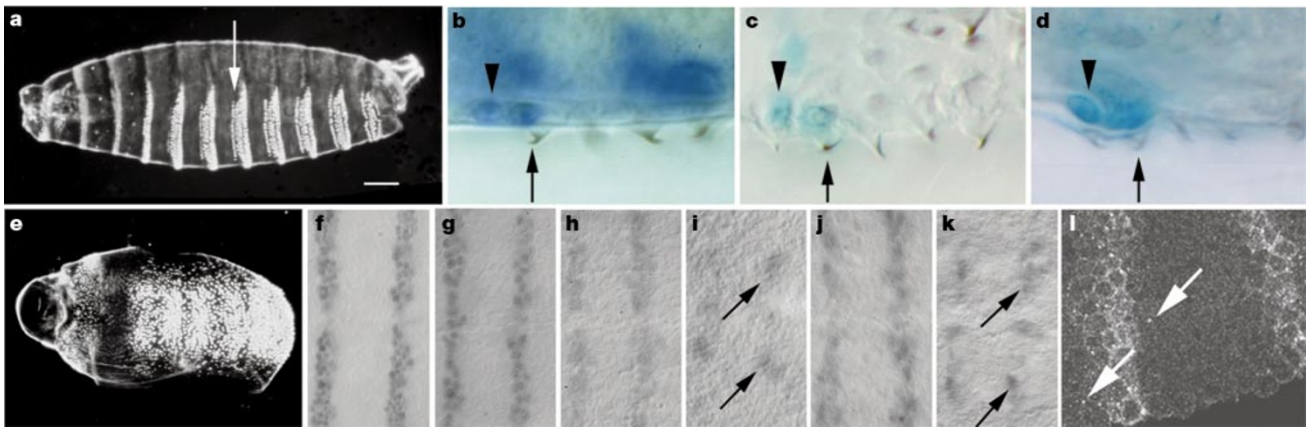

Figure 1 Arrow is required for Wg-dependent cell fates. Shown are larval cuticles, anterior left, ventrolateral (**a**), ventral (**e**–**k**) and optical sections (**b**–**d**). **a**, Wild type (WT); normal segmentation and patterning generates regions of alternating denticle and smooth cuticle. Arrow indicates first denticle row of abdominal segment four. **b**, WT; first four rows of a single denticle belt. Row 1 (arrow) is formed by the posterior of the two overlying En-lacZ-expressing cells (blue; **b**–**d**); the anterior En cell (arrowhead) secretes smooth cuticle. Staining above hypodermis is irrelevant CNS expression. **c**, wg^{ts}, inactivated at 8 hours a.e.l.; the anterior En cell (arrowhead) now produces a denticle. **d**, Zygotic *arrow* mutant; the anterior En cell (arrowhead) now adopts denticle fate. Ectopic denticles are also found just posterior to the belt[30]. **e**, arr^{null} embryo; no smooth cuticle is produced, as in *wg* null mutants (not shown). **f**–**k**, Anti-En monoclonal antibody 4D9 staining of one and a half parasegments of filleted epidermis. **f**, WT, 3.5 hours a.e.l.; En expression is initiated in narrow stripes. **g**, WT, 6 hours a.e.l.; En is maintained. **h**, **i**, *wg* null; En expression is induced normally (**h**) but fades from the epidermis (**i**), although it remains in underlying neuroblasts (arrows). **j**, **k**, arr^{1B}/Df(2R)AA1 maternal and zygyotically mutant embryos; En expression is induced normally (**j**), but fades from the epidermis (**k**), although it remains in underlying neuroblasts (arrows). **l**, Anti-Wg, monoclonal antibody 4D4. arr^{null}, ~4.5 hours a.e.l., one parasegment magnified to visualize Wg protein (arrows) distant from Wg producing cells. Scale bars, 70 μm (**a**); 6 μm (**b**–**d**); 50 μm (**e**); 25 μm (**f**–**k**); 9 μm (**l**).

Initially, *arrow* messenger RNA is distributed uniformly in the embryo, owing to maternal contribution, but by stage 9 broad stripes are superimposed on this global expression (data not shown). As zygotic expression takes over, *arrow* mRNA stripes become more accentuated (Fig. 2d), such that by stage 13 the highest levels are posterior to the En domain, and the lowest levels are just anterior to the En domain, in the region signalled by Wg at this stage (Fig. 2d, dots). Similarly, in leg discs *arrow* transcription is lowest in cells expressing Wg (data not shown). This suggests that *arrow* transcription is negatively regulated by Wg signalling, in a manner similar to the Frizzled receptors Fz and DFz2 (refs 3, 4), but unlike the signal transducers Dsh and Arm, which are both uniformly expressed[5,6]. Although the significance of this transcriptional regulation is unclear, it is unlikely that it is relevant to signalling in the embryo, as global maternal *arrow* contribution suffices for most epidermal Wg signalling events. Polymerase chain reaction with reverse transcription (RT–PCR) analysis shows also that *arrow* mRNA is expressed in S2 cells (data not shown), consistent with these cells being able to respond to Wg once transfected with DFz2 (ref. 3).

arrow encodes a protein of 1,678 amino acids exhibiting a striking sequence conservation to the mammalian LDL-receptor related proteins LRP5 and LRP6 (Fig. 3; 71% similarity, 40% identity[7–10]; a complete alignment is posted at http://www.med.upenn.edu/~cellbio/DiNardo.html; see also Supplementary Information). Arrow is a putative type I transmembrane protein containing four epidermal growth factor (EGF)-like repeats, each preceded by six YWTD spacer domains. Between the EGF/YWTD region and the membrane are LDL-receptor (LDLR) type A repeats. Both classes of repeats have been implicated in ligand binding in other contexts. For example, the LDLR repeats in the LDL receptor are central to binding the LDL particle, whereas EGF-like repeats contribute to ligand binding by some LRPs[11]. The cytoplasmic tail contains proline-rich regions that are potential targets for SH3-domain-containing proteins, and the sequence YKII is a potential signal for internalization. Sequencing of two *arrow* alleles indicates that they are most probably null mutants. In arr^{2} a stop codon is introduced at position 753, between EGF-like repeats 2 and 3 (Fig. 3, asterix; data not shown). Another allele, arr^{134}, was generated by imprecise P-element excision and remove sequences that include the translation start and part of the signal peptide up to codon 57 (in addition to P-element internal sequences).

Arrow, LRP5 and LRP6 form a distinct group of LRPs based on overall sequence conservation (data not shown, see http://www.med.upenn.edu/~cellbio/DiNardo.html). The conservation among Arrow, LRP5 and LRP6 is not restricted to the repeats, but is found throughout the proteins. In addition, the blocks of EGF-like and LDL-receptor repeats are in reversed order as compared with other LRP members. Finally, the EGF-like repeats of Arrow are slightly more closely related to those of LRP5 and LRP6 than to those in other LRP proteins. The same is true for the LDL receptor repeats (data not shown). These comparisons indicate a significant functional conservation between *Drosophila* Arrow and human LRP5 and LRP6.

As Arrow appears not to be involved in production of Wg, Arrow might be required in cells receiving Wg input. To test this, we examined the expression of Wg target genes in tissues mosaic for *arrow* function. If Arrow is required to produce active signal, then *arrow* mutant cells will be rescued by signal produced from adjacent Arrow-positive cells. On the other hand, if Arrow is necessary in the receiving cell, then all the *arrow* mutant cells will exhibit a defect in Wg target gene expression. Wg is expressed along the dorso-ventral boundary of the wing disc. Secreted from these cells, Wg activates the transcription of Distalless (Dll), and acts in a concentration-dependent manner to pattern the wing[12,13]. In the wing pouch, none of the *arrow* mutant cells within a clone expresses Dll (Fig. 4a–d). As mutant cells at the edge of the clone are not rescued by Wg secreted from their wild-type neighbours, *arrow* function is necessary in the cell receiving Wg. This is supported by analysis in the leg disk, where Wg is expressed in a ventral quadrant, and specifies ventral and ventro-lateral fates. Proper patterning also requires that *dpp*, a secreted factor necessary for dorsal and dorso-lateral fates, is repressed in cells receiving Wg. If Wg signal transduction is blocked, as in clones of cells mutant for *dsh* (refs 14–17), *dpp* expression is de-repressed and patterning is disrupted. Similarly, *dpp* expression is de-repressed in clones of cells mutant for *arrow* in the ventral anterior quadrant (Fig 4e–h). These analyses show that *arrow* is necessary in cells responding to Wg input, for both positive and negative gene regulation.

Having established that *arrow* acts in the responding cell, we ordered the requirement for *arrow* relative to the intracellular transduction cascade. Smooth cuticle is restored to arr^{null} embryos in alternate segments when Dsh is expressed using Prd–GAL4, indicating rescue of Wg signal transduction (Fig. 2b). This contrasts with the overexpression of Wg, which had no effect in arr^{null} embryos (data not shown). These data suggest that Arrow acts downstream of Wg but upstream of Dsh, as signalling, once activated by Dsh, no longer requires Arrow. It remains possible that Arrow might normally act as a scaffold and concentrate Dsh to an appropriate subcellular location; in this model, flooding the cell with Dsh simply bypasses the requirement for Arrow. In either case, Arrow is unlikely to act in a pathway parallel to Wg signal transduction as (1) the *arrow* mutant phenotype is rescued by

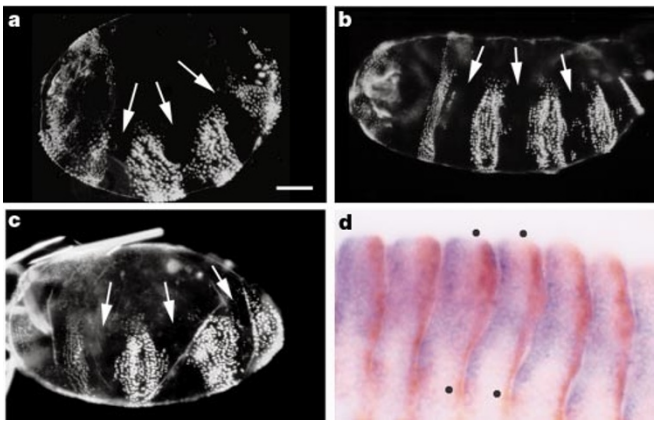

Figure 2 *arr* functions downstream of *wg* but upstream of *dsh*. Ventral (**b**) or ventrolateral (**a**, **c**). **a**, arr^{null} UAS–Arr; Prd–GAL4; smooth cuticle (arrows), indicating restored Wg signalling, now interrupts the lawn of denticles. **b**, arr^{null}; UAS–Dsh/Prd–GAL4; overexpression of Dsh in alternate segments produces smooth cuticle (arrows), indicating restored Wg signalling to this arr^{null} embryo. Similar results were obtained with activated Armadillo (not shown). **c**, wg^{cx4}; UAS–Dsh/Prd–GAL4; overexpression of Dsh in alternate segments produces smooth cuticle (arrows), showing that excess Dsh activates signalling in a ligand-independent manner. **d**, Arrow mRNA *in situ*. WT, stage 13; Arrow mRNA (blue) is expressed at high levels just posterior to En-expressing cells (brown), and at lower levels in regions signalled by Wg (dots). Ventral midline is along panel bottom. Scale bars, 77 μm (**a**–**c**); 30 μm (**d**).

Figure 3 Arrow is a member of the LDL-receptor protein family. Arrow contains four EGF-like repeats (class B2; filled boxes), three LDL receptor repeats (type A; cross-hatching), a transmembrane domain (hatched) and a cytoplasmic tail. SP, signal peptide; bar, 100 amino acids; asterix, stop codon in arr^{2}.

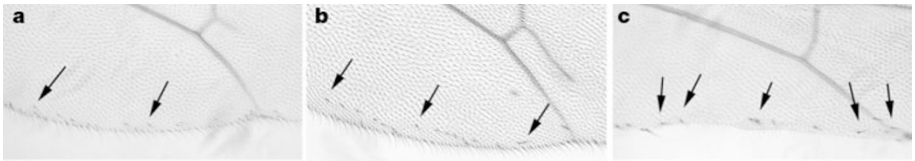

Figure 5 Ectopic expression of Arrow mimics ligand-dependent pathway activation. Adult wings, magnification of posterior margin. Arrows and arrowheads indicate some ectopic margin bristles. **a**, Overexpression of DFz2 generates ectopic margin bristles, in a Wg-dependent fashion[19]. **b**, Similarly, overexpression of Arrow in clones also produces ectopic bristles in the vicinity of the margin. **c**, Wing with *arrow* clones, simultaneously overexpressing DFz2. Loss of *arrow* in clones causes notching, with loss of margin bristles; yet, overexpression of DFz2 (as in **a**), rescues neither any *arrow* mutant tissue nor mutant bristles (marked by *yellow*). A large notch resulting from loss of *arrow* function is apparent, yet all bristles found nearby (arrows) are generated from wild-type tissue.8

Dsh, a canonical Wg signal transducer, and (2) loss of *arrow* function blocks signalling even when excess Wg is presented. In addition, the fact that the *arrow* phenotype is not suppressed by excess Wg distinguishes *arrow* from the genes involved in proteoglycan-assisted presentation of the Wg ligand. Each of the mutants affecting this step, *sugarless*, *sulfateless* and *dally*, is substantially suppressed by providing excess Wg ligand, showing that glycosaminoglycans are not essential for reception of the signal but only increase the efficiency of ligand presentation to the receptor (ref. 18 and references therein). Together, these data argue that Arrow is absolutely essential for Wg to signal, and are consistent with a role for Arrow in reception rather than presentation of signal.

The mosaic and epistasis analyses place the requirement for Arrow activity upstream of Dishevelled in responding cells. Because *arrow* encodes a putative transmembrane protein, epistasis tests between Arrow and Fz proteins would be of interest, but no activating mutations exist in either Fz or Arrow that would lead to signal transduction in the absence of ligand. There are, however, several suggestive similarities between Fz proteins and Arrow. Arrow and DFz2 transcription is modulated similarly, whereas that of the Dsh and Arm signal transducers is not. In addition, ectopic DFz2 expression can mildly sensitize cells to Wg signalling, for example in the wing, where overexpression of DFz2 produces ectopic margin bristles—a Wg-dependent cell type[19] (Fig. 5a). This potentiation of Wg signalling is ligand-dependent, and ectopic bristles are only found near the wing margin, which is a source of high levels of Wg[19]. As is expected for a gene essential for Wg signalling, loss of *arrow* function in clones leads to loss of margin (data not shown; see Fig. 5c), similar to that observed for *fz Dfz2* clones[20]. We find that overexpression of Arrow also produces ectopic bristles near the wing margin (Fig. 5b). Thus, *arrow* is required for Wg-dependent signalling at the margin, and can potentiate Wg signalling in a manner similar to that of DFz2. We also find that the potentiation of signalling caused by excess DFz2 depends on *arrow* function, as shown by inducing *arrow* mutant clones while overexpressing DFz2 (Fig. 5c). If excess DFz2 were able to bypass Arrow and restore signalling on *arrow* mutant cells then these cells should retain the ability to form wing margin and produce marked *arrow* mutant margin bristles, neither of which was observed. This result is consistent either with Arrow functioning after DFz2 engages ligand, or with Arrow and the Fz class proteins functioning as co-receptors, although this epistasis must be confirmed when activating mutations become available.

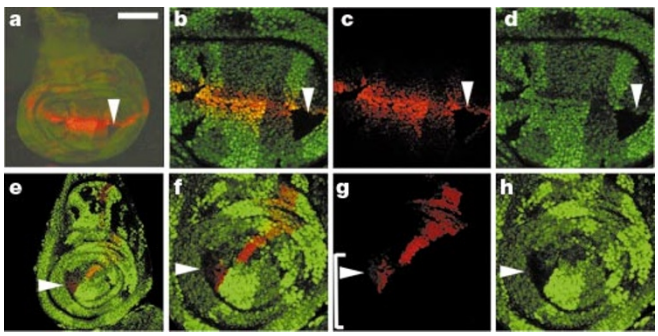

Figure 4 *arrow* is required cell-autonomously for Wg target gene expression. **a**–**h**, Homozygous arr^{null} clones marked by the absence of pi-Myc marker (green). Heterozygous tissue stains at intermediate levels, whereas the homozygous wild-type twin spot containing two copies of pi-Myc stains more brightly. **a**, Dll–LacZ expression (red) in wing disc, magnified in **b**–**d**; dorsal is up. Dll expression is lost in arr^{null} clones at the dorso–ventral boundary (arrowhead, **a**–**c**). Note the stronger Dll expression in wild-type twin spots compared with heterozygous tissue, indicating an *arrow* gene-dosage effect on the efficiency of Wg signal transduction. **e**, Dpp–LacZ expression (red), magnified in **f**–**h**; anterior is to the left, dorsal up. Dpp expression is induced in anterior compartment cells by Hh signalling from the posterior compartment. Wg signalling, active in ventral anterior sectors, represses *dpp*, so that high-level Dpp expression is normally restricted to a stripe of cells located dorsally along the antero-posterior compartment border. An *arr* clone (arrowhead) in the ventral, anterior sector (Fig. 4g, bracket), near the compartment boundary, now expresses Dpp–LacZ ectopically. Expression is weaker in mutant cells more distant from the Hh-expressing source, similar to the graded endogenous Dpp expression observed dorsally. Scale bars, 80 μm (**a**); 35 μm (**b**–**d**); 65 μm (**e**); 35 μm (**f**–**h**).

The extensive homology between Arrow and both mouse and human LRP5 and LRP6, indicates that the role we ascribe to Arrow in Wg signalling may extend to these LRPs for Wnt signalling. Indeed, an insertion in the mouse LRP6 gene has been identified that leads to several Wnt-like phenotypes[21]. Our work suggests that Arrow, and by extension LRP5 and LRP6, have specific roles for the Wg/Wnt pathway, as both Dpp and Hh can signal to *arrow* null cells (S.T.D. and S.D., unpublished data)[22]. We find that *arrow* null mutant cells do not survive as well as their wild-type sister cells when twin spot clones are made, suggesting some role in viability (S.T.D. and S.D., unpublished data) (see also Fig. 5c). Whether this can be attributed to a deficit in Wnt signalling is not known, although cells doubly mutant for *fz* and *dfz2* also do not survive[20].

Our simplest model is that Arrow and a Fz-class protein act together as a receptor complex. Some support for this is presented in an accompanying paper[23]. Alternatively, Arrow might assist in recycling the Fz receptors to the plasma membrane after Wg/Wnt ligand binding and internalization, thereby providing unoccupied receptors to allow efficient, extended signalling. This idea is suggested by the fact that Arrow is related to LDL receptors, which are sometimes involved in recycling proteins from the plasma membrane. If this were the case, then overexpression of Fz proteins should suppress the need for *arrow* function by supplying excess nascent receptors. However, overexpressing DFz2 at the wing margin did not suppress the Wg signalling defect caused by loss of *arrow* function.

As several components required for Wg signalling, such as Dsh, Sgg and Fz, are also necessary for the determination of tissue polarity (reviewed in ref. 24), we tested whether Arrow also acts in this process. The only tissue where we observed polarity defects is the eye. However, the role for Arrow in polarity in this tissue is probably indirect, reflecting an early, global role for a Wnt pathway upstream of planar polarity determination[22]. In other tissues, Arrow is not involved in tissue polarity. For example, *arr* mutant clones in

the dorsal leg exhibit no such defects (data not shown). This result also shows that the Fz receptor is available to respond to tissue polarity signals in the absence of *arrow* function and one would therefore expect it to be at the cell surface in *arrow* mutant cells. This finding suggests that Arrow does not merely act as a chaperone to guide Fz-class proteins to the cell surface. This again is consistent with our model that Fz and Arrow have a similar role in the reception of the Wg signal and that they may both be part of a single receptor complex. Recent work raises the possibility that other LRPs are part of a signal reception complex, just as we postulate for Arrow. The VLDL and ApoE receptors (both LRPs) are essential during mouse cerebellar development, where they bind the ligand, Reelin, while intracellularly binding to, and inducing the phosphorylation of, the adapter protein, Disabled-1 (reviewed in ref. 25). In addition to the LRPs, a second receptor—the Cadherin-related neuronal receptor—also binds Reelin, while its intracellular domain associates with the Fyn tyrosine kinase. This suggests that as the two receptor subunits bind Reelin, two proteins are brought into proximity inside the cell, Disabled-1 and Fyn[26]. Perhaps Arrow and the Fz proteins similarly bind ligand and consequently bring together proteins in the cytoplasm that initiate Wg/Wnt signalling. □

Methods

Two cDNAs, corresponding to CT15575, isolated from a 0-4h library[27] contained an open reading frame preceded by stop codons in all frames. Two ATGs are found 5′ to a putative signal peptide. For UAS–Arrow, cDNA F1 from pNB40 was cloned into pUASg as a *XhoI*/partial *Not*I fragment.

arr^{2} germline clones[28] were induced in HS-Flp/+; FRT42B *arr*^{2}/FRT42B *ovo*^{D1} females mated to Df(2R)8-104/CyO or Df(2R)AA1/CyO Hb-lacZ males, and null embryos were identified by absence of Hb-lacZ staining. Disc clones were induced in *y w* hs-Flp; *dpp*^{10638} (or Dll–LacZ) FRT43D *arr*^{2}/FRT43D pi-Myc (45F, 47F) larvae[29]. Confocal projections were captured with LSM510 software on a Zeiss axiovert microscope. For adult wings, MS1096–GAL4 was used to express UAS–DFz2 (ref. 19), or UAS-FRT-white+FRT-Arrow. Flies analysed were of genotype *y w* hs-flipase MS1096/ *y w*; UAS-DFz2/+ *y w* hs-flipase MS1096/ *w*; Df(2)8-104 UAS-FRT white+ FRT-Arrow /+, where the white+FRT cassette was removed in clones after heat-shock-induced flipase recombination[22]. Marked *arr* clones were induced while overexpressing DFz2 in *y w* hs-flipase MS1096/ *y w*; FRT42D *arr*^{2}/ FRT42D y+ w+; UAS-DFz2/+ flies.

Received 21 January; accepted 2 August 2000.

1. Wodarz, A. & Nusse, R. Mechanisms of Wnt signalling in development. *Annu. Rev. Cell Dev. Biol.* **14,** 59–88 (1998).
2. Dougan, S. T. & DiNardo, S. *wingless* generates cell type diversity among *engrailed* expressing cells. *Nature* **360,** 347–350 (1992).
3. Bhanot, P. *et al.* A new member of the *frizzled* family from *Drosophila* functions as a Wingless receptor. *Nature* **382,** 225–230 (1996).
4. Müller, H., Samanta, R. & Wieschaus, E. Wingless signalling in the *Drosophila* embryo: zygotic requirements and the role of the frizzled genes. *Development* **126,** 577–586 (1999).
5. Klingensmith, J., Nusse, R. & Perrimon, N. The *Drosophila* segment polarity gene *dishevelled* encodes a novel protein required for response to the *wingless* signal. *Genes Dev.* **8,** 118–130 (1994).
6. Riggleman, B., Schedl, P. & Wieschaus, E. Spatial expression of the *Drosophila* segment polarity gene armadillo is posttranscriptionally regulated by *wingless*. *Cell* **63,** 549–560 (1990).
7. Hey, P. J. *et al.* Cloning of a novel member of the low–density lipoprotein receptor family. *Gene* **216,** 103–111 (1998).
8. Kim, D. H. *et al.* A new low density lipoprotein receptor related protein, LRP5, is expressed in hepatocytes and adrenal cortex, and recognizes apolipoprotein E. *J. Biochem. (Tokyo)* **124,** 1072–1076 (1998).
9. Dong, Y. *et al.* Molecular cloning and characterization of LR3, a novel LDL receptor family protein with mitogenic activity. *Biochem. Biophys. Res. Commun.* **251,** 784–790 (1998).
10. Chen, D., Lathrop, W. & Dong, Y. Molecular cloning of mouse Lrp7(Lr3) cDNA and chromosomal mapping of orthologous genes in mouse and human. *Genomics* **55,** 314–321 (1999).
11. Brown, M. S., Herz, J. & Goldstein, J. L. LDL-receptor structure. Calcium cages, acid baths and recycling receptors. *Nature* **388,** 629–630 (1997).
12. Zecca, M., Basler, K. & Struhl, G. Direct and long-range action of a wingless morphogen gradient. *Cell* **87,** 833–844 (1996).
13. Neumann, C. J. & Cohen, S. M. Long–range action of Wingless organizes the dorsal–ventral axis of the *Drosophila* wing. *Development* **124,** 871–880 (1997).
14. Brook, W. J. & Cohen, S. M. Antagonistic interactions between *wingless* and *decapentaplegic* responsible for dorsal–ventral pattern in the *Drosophila* leg. *Science* **273,** 1373–1377 (1996).
15. Jiang, J. & Struhl, G. Complementary and mutually exclusive activities of *decapentaplegic* and *wingless* organize axial patterning during *Drosophila* leg development. *Cell* **86,** 401–409 (1996).
16. Penton, A. & Hoffmann, F. M. *Decapentaplegic* restricts the domain of *wingless* during *Drosophila* limb patterning. *Nature* **382,** 162–164 (1996).
17. Heslip, T. R., Theisen, H., Walker, H. & Marsh, J. L. Shaggy and dishevelled exert opposite effects on Wingless and Decapentaplegic expression and on positional identity in imaginal discs. *Development* **124,** 1069–1078 (1997).
18. Perrimon, N. & Bernfield, M. Specificities of heparan sulphate proteoglycans in developmental processes. *Nature* **404,** 725–728 (2000).
19. Cadigan, K. M., Fish, M. P., Rulifson, E. J. & Nusse, R. Wingless repression of *Drosophila* frizzled 2 expression shapes the Wingless morphogen gradient in the wing. *Cell* **93,** 767–777 (1998).
20. Chen, C. & Struhl, G. Wingless transduction by the frizzled and frizzled2 proteins of *Drosophila*. *Development* **126,** 5441–5452 (1999).
21. Pinson, K., Brennan, J., Monkley, S., Avery, B. & Skarnes, W. C. An LDL-receptor-related protein, regulates Wnt signalling in mice. *Nature* **407,** 535–538 (2000).
22. Wehrli, M. & Tomlinson, A. Independent regulation of anterior/posterior and equatorial/polar polarity in the *Drosophila* eye; evidence for the involvement of Wnt signalling in the equatorial/polar axis. *Development* **125,** 1421–1432 (1998).
23. Tamai, K. *et al.* LDL-receptor-related proteins in Wnt signal transduction. *Nature* **407,** 530–535 (2000).
24. Axelrod, J. D., Miller, J. R., Shulman, J. M., Moon, R. T. & Perrimon, N. Differential recruitment of Dishevelled provides signalling specificity in the planar cell polarity and Wingless signalling pathways. *Genes Dev.* **12,** 2610–2622 (1998).
25. Rice, D. S. & Curran, T. Mutant mice with scrambled brains: understanding the signalling pathways that control cell positioning in the CNS. *Genes Dev.* **13,** 2758–5873 (1999).
26. Senzaki, K., Ogawa, M. & Yagi, T. Proteins of the CNR family are multiple receptors for Reelin. *Cell* **99,** 635–647 (1999).
27. Brown, N. H. & Kafatos, F. C. Functional cDNA libraries from *Drosophila* embryos. *J. Mol. Biol.* **203,** 425–437 (1988).
28. Chou, T. B., Noll, E. & Perrimon, N. Autosomal P[ovoD1] dominant female-sterile insertions in *Drosophila* and their use in generating germ-line chimeras. *Development* **119,** 1359–1369 (1993).
29. Wehrli, M. & Tomlinson, A. Epithelial planar polarity in the developing *Drosophila* eye. *Development* **121,** 2451–2459 (1995).
30. Nüsslein–Volhard, C., Wieschaus, E. & Kluding, H. Mutations affecting the pattern of the larval cuticle in *Drosophila melanogaster I* Zygotic loci on the second chromosome . *Roux's Arch. Dev. Biol.* **193,** 267–282 (1984).

Supplementary information is available on *Nature*'s World-Wide Web site (http://www.nature.com) or from http://www.med.upenn.edu/~cellbio/DiNardo.html or as paper copy from the London editorial office of *Nature*.

Acknowledgements

G. Campbell, G. Struhl, F. Diaz-Benjumea, S. Cohen, R. Goto-Mandeville, E. Bieschke and B. Calvi provided insightful suggestions and help along the way. The free exchange of information with the Skarnes lab is acknowledged. The manuscript was improved by comments from N. Erdeniz, P. Klein, B. Wilder and the DiNardo lab. Material provided by J. Szidonya, the Bloomington Stock Center and Berkeley Drosophila Genome Project was of great importance. Supported by the Swiss National Science Foundation (M.W.), NIH (A.T. and S.D.) and American Cancer Society (S.D.).

Correspondence and requests for materials should be addressed to S.D. (e-mail: sdinardo@mail.med.upenn.edu).

LDL-receptor-related proteins in Wnt signal transduction

Keiko Tamai*, Mikhail Semenov*, Yoichi Kato*, Rebecca Spokony†, Chunming Liu*, Yu Katsuyama*, Fred Hess‡, Jean-Pierre Saint-Jeannet† & Xi He*

* *Division of Neuroscience, Children's Hospital, Department of Neurology, Harvard Medical School, 300 Longwood Avenue, Boston, Massachusetts 02115, USA*
† *Department of Animal Biology, School of Veterinary Medicine, University of Pennsylvania, 3800 Spruce Street, Philadelphia, Pennsylvania 19104, USA*
‡ *Department of Human Genetics, Merck Research Laboratories, PO Box 4, West Point, Pennsylvania 19486, USA*

The Wnt family of secreted signalling molecules are essential in embryo development and tumour formation[1]. The Frizzled (Fz) family of serpentine receptors function as Wnt receptors[2–10], but how Fz proteins transduce signalling is not understood. In *Drosophila*, *arrow* phenocopies the *wingless* (DWnt-1) phenotype[11], and encodes a transmembrane protein[11] that is homologous to two members of the mammalian low-density lipoprotein receptor (LDLR)-related protein (LRP) family, LRP5 and LRP6 (refs 12–15). Here we report that LRP6 functions as a co-receptor for Wnt signal transduction. In *Xenopus* embryos, LRP6 activated

Labelling of purified sGC

sGC (12.5 μg; purity about 91%) was dissolved in PAL buffer (50 mM TEA-HCl, 0.1 mM EGTA, 1 mM cGMP, 3 mM $MgCl_2$, 200 μM GTP, pH 7.4) and incubated with 20 μCi ^{3}H-PAL (25 μM) in the presence or absence of different sGC modulators (5 min, 37 °C). Samples were irradiated at 254 nM (N8K ultraviolet 254-nM hand lamp, CAMAG, Berlin, Germany; distance 30 mm, 20 °C, 15 min) and the reaction was stopped by adding SDS-containing stop solution (312.5 mM Tris-HCl, 10% (w/v) SDS, 50% (v/v) glycerol, 250 mM dithiothreitol (DTT), 0.025% (w/v) bromophenol blue, pH 6.8) and heating (5 min at 80 °C). For control 12.5 μg sGC was incubated with 20 μCi ^{3}H-PAL without irradiation. Separation was performed on a 7.5% SDS–PAGE (Protean II cell; Bio-Rad, München, Germany) using a modified Laemmli method[27]. Proteins were fixed for 20 min in 30/10/60 methanol/acetic acid/MilliQ water, dried and exposed to BAS-TR 20/25 imaging plates (Fuji Photo Film; Tokyo, Japan) for 15 days[28]. After exposure, the Imaging Plates were scanned by means of a laser scanner (BAS 5000 Scanner; RayTest, Straubenhardt, Germany). Evaluation was performed by visual classification of radiographic intensities, displayed by use of pseudo-colours, starting with blue for lowest detectable concentrations up to red for highest concentrations.

CNBr fragmentation of labelled sGC

sGC (200 μg) was labelled with 1,600 μCi ^{3}H-meta-PAL, and the reaction was terminated by adding TCA to a final concentration of 10%. The protein was precipitated, washed with ice-cold ethanol/ether (1/1), dissolved in formic acid (70% (v/v)) and reacted with a few crystals of CNBr in the dark (24 h, 20 °C) under oxygen-free nitrogen. After evaporation in a Speed Vac (Bachofer, Reutlingen, Germany) for three times after the addition of 1 ml MilliQ water, the pellet was dissolved in sample buffer (62.5 mM Tris-HCl, 2% (w/v) SDS, 10% (v/v) glycerol, 50 mM DDT, 0.0025 % (w/v) bromophenol blue, pH 6.8) heated (5 min, 80°C), and the protein fragments were separated on a 10–20% gradient SDS–PAGE or a 16.5% Tris-Tricine gel. The digested protein fragments were transferred to a PVDF membrane (Trans-Blot Electrophoretic Transfer Cell; Bio-Rad) and stained with Coomassie blue. Dried membranes were exposed to BAS-TR 20/25 Imaging Plates for 6 h without (10–20% gradient gel blot) or for 48 h with a screen of metal folio for contamination monitors (0.9 mg cm^{-2} Steiner; Erndtebrück-Schameder, Germany) (16.5% Tris-Tricine gel blot).

Amino-terminal sequence analysis

Amino-terminal sequence analyses were performed using the gas-liquid-solid-phase protein sequencer Procise with an RP-18-PTH-column from Applied Biosystems (Forster City, CA, USA).

Sequence analysis

PVDF-membrane pieces were washed two times with 100 μl of 50% MeOH before sequencing. The cyanogen bromide fragment VIII was sequenced over 60 cycles using the sequencer program for blot sequencing. The single PTH-amino-acids were collected, lyophilized and radioactivity was counted after combustion (Oxidizer model 307, Oximate 80; Packard, Illinois, USA) in a liquid scintillation counter (LS-6500; Beckman, Munich, Germany)

Statistics

Results are given as the mean ± s.e.m. Differences were assessed by one-way analysis of variance (ANOVA) followed by Bonferoni test for comparison of means.

Received 18 April; accepted 11 December 2000.

1. Moncada, S., Palmer, R. M. & Higgs, E. A. Nitric oxide: physiology, pathophysiology, and pharmacology. *Pharmacol. Rev.* **43,** 109–142 (1991).
2. Furchgott, R. F. Endothelium-derived relaxing factor: Discovery, early studies, and identification as nitric oxide (Nobel lecture). *Angew. Chem. Int. Ed. Engl.* **38,** 1870–1880 (1999).
3. Murad, F. Discovery of some of the biological effects of nitric oxide and its role in cell signaling (Nobel lecture). *Angew. Chem. Int. Ed. Engl.* **38,** 1857–1868 (1999).
4. Ignarro, L. J. Nitric oxide: A unique endogenous signaling molecule in vascular biology (Nobel lecture). *Angew. Chem. Int. Ed. Engl.* **38,** 1882–1892 (1999).
5. Straub, A. *et al.* Substituted pyrazole derivatives. WO 2,000,006,568 (2000). *Chem. Abstr.* **132,** 122629 (2000)
6. Garthwaite, J. *et al.* Potent and selective inhibition of nitric oxide-sensitive guanylyl cyclase by 1H[1,2,4]oxadiazolo[4,3-a]quinoxalin-1-one. *Mol. Pharmacol.* **48,** 184–188 (1995).
7. Schrammel, A., Behrends, S., Schmidt, K., Koesling, D. & Mayer, B. Characterization of 1H[1,2,4]oxadiazolo[4,3-a]quinoxalin-1-one as a heme-site inhibitor of nitric oxide-sensitive guanylyl cyclase. *Mol. Pharmacol.* **50,** 1–5 (1996).
8. Brunner, F., Schmidt, K., Nielsen, E. B. & Mayer, B. Novel guanylyl cyclase inhibitor potently inhibits cyclic GMP accumulation in endothelial cells and relaxation of bovine pulmonary artery. *J. Pharmacol. Exp. Ther.* **277,** 48–53 (1996).
9. Friebe, A., Schultz G. & Koesling, D. Sensitizing soluble guanylate cyclase to become a highly CO-sensitive enzyme. *EMBO J.* **15,** 6863–6868 (1996).
10. Hoenicka, M. *et al.* Purified soluble guanylyl cyclase expressed in a baculovirus/Sf9 system: stimulation by YC-1, NO and CO. *J. Mol. Med.* **77,** 14–23 (1999).
11. Nakane, M. *et al.* Molecular cloning and expression of cDNAs coding for soluble guanylate cyclase from rat lung. *J. Biol. Chem.* **265,** 16841–16845 (1990).
12. Zabel, U., Weeger, M., La, M. & Schmidt, H. H. H. W. Human soluble guanylate cyclase: functional expression and revised isoenzyme family. *Biochem. J.* **335,** 51–57 (1998).
13. Stasch, J. P., Kazda, S. & Neuser, D. Different effects of ANP and nitroprusside on cyclic GMP extrusion of isolated aorta. *Eur. J. Pharmacol.* **174,** 279–282 (1989).
14. Becker, E. M. *et al.* The vasodilator-stimulated phosphoprotein (VASP): target of YC-1 and nitric oxide effects in human and rat platelets. *J. Cardiovasc. Pharmacol.* **35,** 390–397 (2000).
15. Mülsch, A. *et al.* Effect of YC-1, an NO-independent, superoxide-sensitive stimulator of soluble guanylyl cyclase, on smooth muscle responsiveness to nitrovasodilators. *Br. J. Pharmacol.* **120,** 681–689 (1997).
16. Ko, F. N., Wu, C. C., Kuo, S. C., Lee, F. Y. & Teng, C. M. YC-1, a novel activator of platelet guanylate cyclase. *Blood* **84,** 4226–4233 (1994).
17. Wu, C. C., Ko, F. N., Kuo, S. C., Lee, F. Y. & Teng, C. M. YC-1 inhibited human platelet aggregation through NO-independent activation of soluble guanylate cyclase. *Br. J. Pharmacol.* **116,** 1973–1978 (1995).
18. Becker, E. M. *et al.* Generation and characterization of a stable soluble guanylate cyclase-over-expressing CHO cell line. *Nitric Oxide* **3,** 55–66 (1999).
19. Friebe, A. & Koesling, D. Mechanism of YC-1 induced activation of soluble guanylyl cyclase. *Mol. Pharmacol.* **53,** 123–127 (1998).
20. Hobbs, A. J. Soluble guanylate cyclase: the forgotten sibling. *Trends Pharmacol. Sci.* **18,** 484–491 (1997).
21. Galle, J. *et al.* Effects of the soluble guanylyl cyclase activator, YC-1, on vascular tone, cyclic GMP levels and phosphodiesterase activity. *Br. J. Pharmacol.* **127,** 195–203 (1999).
22. Hirth-Dietrich, C., Stasch, J. P. & Ganten, D. Transgenic rats with an additional renin gene (TGR(mRen2)27) as a sensitive model for the renal effects of NO synthase inhibition. *Naunyn-Schmiedeberg's Arch. Pharmacol.* **350,** R6 (1994).
23. Zhao, Y., Schelvis, J. P. M., Babcock, G. T. & Marletta, M. A. Identification of histidine 105 in the β1 subunit of soluble guanylate cyclase as the heme proximal ligand. *Biochemistry* **37,** 4502–4509 (1998).
24. Zhao, Y. & Marletta, M. A. Localization of the heme binding region in soluble guanylate cyclase. *Biochemistry* **36,** 15959–15964 (1997).
25. Kharitonov, V. G., Sharma, V. S., Magde, D. & Koesling, D. Kinetics and equilibria of soluble guanylate cyclase ligation by CO: effect of YC-1. *Biochemistry* **38,** 10699–10706 (1999).
26. Born, G. V. R. & Cross, M. J. The aggregation of blood platelets. *J. Physiol. (Lond.)* **168,** 178–185 (1963).
27. Laemmli, U. K. Cleavage of structural proteins during the assembly of the head of bacteriophage T4. *Nature* **227,** 680–685 (1970).
28. Ahr, H. H. & Steinke, W. Vasodilation and first experience with quantitative studies in whole-body autoradiography during drug development. *Xenobiotic Metab. Dispos.* **9,** 371–378 (1994).

Supplementary information is available on *Nature*'s World-Wide Web site (http://www.nature.com) or as paper copy from the London editorial office of *Nature*.

Acknowledgements

We thank C. Robyr-Fürstner for the synthesis of YC-1; E. Bischoff for performing the PDE assays; and D. Wood for critical comments on the manuscript.

Correspondence and requests for materials should be addressed to J.-P.S. (e-mail: johannes-peter.stasch.js@bayer-ag.de).

Polo-like kinase 1 phosphorylates cyclin B1 and targets it to the nucleus during prophase

Fumiko Toyoshima-Morimoto*†, Eri Taniguchi†, Nobuko Shinya‡, Akihiro Iwamatsu‡ & Eisuke Nishida*†

** Department of Biophysics, Graduate School of Science, Kyoto University, Sakyo-ku, Kyoto 606-8502, Japan*
† Department of Cell and Developmental Biology, Graduate School of Biostudies, Kyoto University, Sakyo-ku, Kyoto 606-8502, Japan
‡ Central Laboratories for Key Technology, Kirin Brewery Company Limited, Kanazawa-ku, Yokohama-shi, Kanagawa 236-0004, Japan

In vertebrate cells, the nuclear entry of Cdc2–cyclin B1 (MPF[1–3]) during prophase[4–6] is thought to be essential for the induction and coordination of M-phase events[7–12]. Phosphorylation of cyclin B1 is central to its nuclear translocation[8,13,14], but the kinases that are responsible remain unknown. Here we have purified a protein kinase from *Xenopus* M-phase extracts that phosphorylates a crucial serine residue (S147) in the middle of the nuclear export signal sequence[10,13,15] of cyclin B1. We have identified this kinase as Plx1 (ref. 16), a *Xenopus* homologue of Polo-like kinase (Plk)-1 (refs 17, 18). During cell-cycle progression in HeLa cells, a change in the kinase activity of endogenous Plk1 toward S147 and/or S133

correlates with a kinase activity in the cell extracts. An anti-Plk1 antibody depletes the M-phase extracts of the kinase activity toward S147 and/or S133. An anti-phospho-S147 antibody reacts specifically with cyclin B1 only during G2/M phase. A mutant cyclin B1 in which S133 and S147 are replaced by alanines remains in the cytoplasm, whereas wild-type cyclin B1 accumulates in the nucleus during prophase. Co-expression of constitutively active Plk1 stimulates nuclear entry of cyclin B1. Our results indicate that Plk1 may be involved in targeting MPF to the nucleus during prophase.

When vertebrate cells enter prophase, cyclin B1 translocates from the cytoplasm to the nucleus[4,5,19]. One of the putative roles of nuclear MPF as the nuclear lamin kinase is crucial for nuclear envelope breakdown at the end of prophase[20]. Four serine residues (S94, S96, S101 and S113) of *Xenopus* cyclin B1 have been identified as *in vivo* phosphorylation sites during the G2/M transition[21,22], and their phosphorylation is thought to be responsible for both nuclear entry of cyclin B1 and germinal vesicle breakdown[8,13,14,22].

When an haemagglutinin A (HA)-tagged mutant of human cyclin B1, in which four serine residues (S126, S128, S133, S147) were replaced by alanine (S126,128,133,147A-cyclin B1), was co-expressed with Myc-tagged wild-type cyclin B1 in HeLa cells, the mutant cyclin B1 remained in the cytoplasm, whereas the wild type accumulated in the nucleus in prophase (Fig. 1a, middle). Myc-tagged wild-type cyclin B1 was indistinguishable from HA-tagged wild-type cyclin B1 in nuclear accumulation during prophase (Fig. 1a, top). This result is consistent with a report that a non-phosphorylatable form of cyclin B1 can enter the nucleus only after nuclear envelope breakdown[14]. Not only S126,128,133,147A-cyclin B1, but also S133,147A-cyclin B1 remained in the cytoplasm during prophase, whereas wild-type cyclin B1 accumulated in the nucleus (Fig. 1a, bottom). S126,128A-cyclin B1 was not exclusively cytoplasmic, and localized, but not accumulated, in the nucleus during prophase (data not shown).

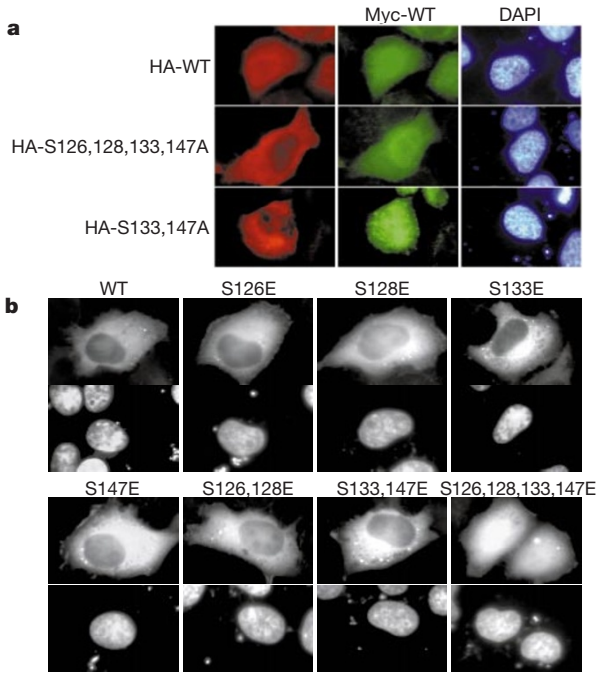

Figure 1 Phosphorylation-dependent nuclear localization of cyclin B1. **a**, Myc-tagged or HA-tagged wild-type (WT) cyclin B1, HA–S126,128,133,147A-cyclin B1, or HA–S133,147A-cyclin B1 were co-expressed in HeLa cells. An image of a prophase cell is shown. **b**, Top, subcellular localization of the indicated forms of HA–cyclin B1 (top). Bottom, DAPI staining. Quantification of staining in the cells is as follows, where N > C indicates staining intensity in the nucleus (N) is stronger than that in the cytoplasm (C); N = C indicates N is equal to C; and N < C indicates C is stronger than N. WT (total 202 cells): N > C, 0; N = C, 1; N < C, 201. S126E (total 158 cells): N > C, 0; N = C, 1; N < C, 157. S128E (total 185 cells): N > C, 0; N = C, 0; N < C, 185. S133E (total 164 cells): N > C, 0; N = C, 0; N < C, 164. S147E (total 190 cells): N > C, 0; N = C, 2; N < C, 188. S126,128E (total 202 cells): N > C, 0; N = C, 21; N < C, 181. S133,147E (total 203 cells): N > C, 1; N = C, 17; N < C, 185. S126,128,133,147E (total 229 cells): N > C, 204; N = C, 20; N < C, 5.

We constructed a series of mutant forms of cyclin B1, in which these four serines were replaced by glutamate to mimic phosphorylation. When each of the serines, or the first two or the last two, were replaced by glutamate, cyclin B1 remained in the cytoplasm (Fig. 1b, S126E,S128E,S133E,S147E,S126,128E and S133,147E). When all four serines were replaced by glutamate, cyclin B1 localized in the nucleus (Fig. 1b, S126,128,133,147E). Together, these results suggest that phosphorylation of S133 and S147 is necessary for the nuclear translocation of cyclin B1 during prophase, and that phosphorylation of S126 and S128 may stimulate the nuclear translocation.

MPF itself can phosphorylate the first two serines[14,21,23], although it has not been proved that MPF regulates nuclear localization of cyclin B1. As our above results showed the importance of identifying a protein kinase(s) that phosphorylates the last two serines, we prepared extracts from synchronized HeLa cells and assayed them for kinase activities toward the various forms of cyclin B1. Kinase activity toward S126,128A-cyclin B1 and toward wild-type cyclin B1 increased roughly in parallel with the activity of MPF—assayed by histone H1 kinase activity—and decreased slightly later than that of MPF (Fig. 2a). Kinase activities toward S126,128,133,147A-cyclin B1 were not observed (Fig. 2a). Thus, a kinase activity that phosphorylates S133 and/or S147 of cyclin B1 becomes activated during G2/M transition in HeLa cells.

U0126, a specific inhibitor of mitogen-activated protein (MAP) kinase kinase MEK at a concentration enough to inhibit epidermal growth factor (EGF)-induced activation of MAP kinase ERK in HeLa cells, did not block the kinase activity of the extracts toward S126,128A-cyclin B1 (Fig. 2b). This indicates that MAP kinase may not be involved in phosphorylating S133 and/or S147 of cyclin B1 during G2 and M phases in HeLa cells. A kinase activity toward S126,128A-cyclin B1 was also detected in the process of *Xenopus* oocyte maturation and found to increase after progesterone treatment (Fig. 2c). Thus, a kinase activity that phosphorylates S133 and/or S147 of cyclin B1 is also activated during G2/M transition in *Xenopus* oocyte maturation.

We purified from *Xenopus* M-phase extracts a kinase activity

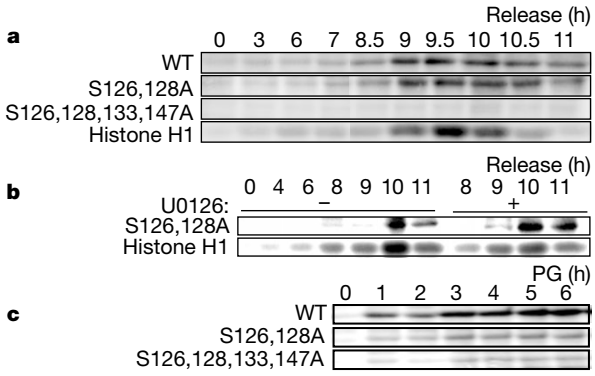

Figure 2 A kinase activity that phosphorylates S133 and/or S147 of cyclin B1 is activated during the G2/M transition. **a**, **b**, Kinase activities in the extracts from synchronized HeLa cells by a double thymidine block[20] toward the indicated substrates. At 6 h after release, U0126 (10 μM) was added in the assays in **b**. **c**, Stage VI *Xenopus* oocytes were treated with progesterone (PG). Oocyte extracts were prepared at the indicated times after treatment with progesterone and the kinase activities in the extracts were measured as in **a**.

toward S126,128A-cyclin B1, which eluted in the flow-through fraction after chromatography on Q-Sepharose (Fig. 3a). We purified the flow-through fraction by sequential chromatography on glutathione *S*-transferase (GST)–cyclinB1–Sepharose, heparin–Sepharose and oligo(dT)–cellulose; and in all steps the kinase activity toward S126,128A-cyclin B1 eluted as a single peak (Fig. 3b and Table 1). Elution of a polypeptide of relative molecular mass 65,000 (M_r 65K), the main band detected by silver staining, coincided completely with that of the kinase activity in the final step (Fig. 3b, Oligo(dT)-Cellulose, top and bottom).

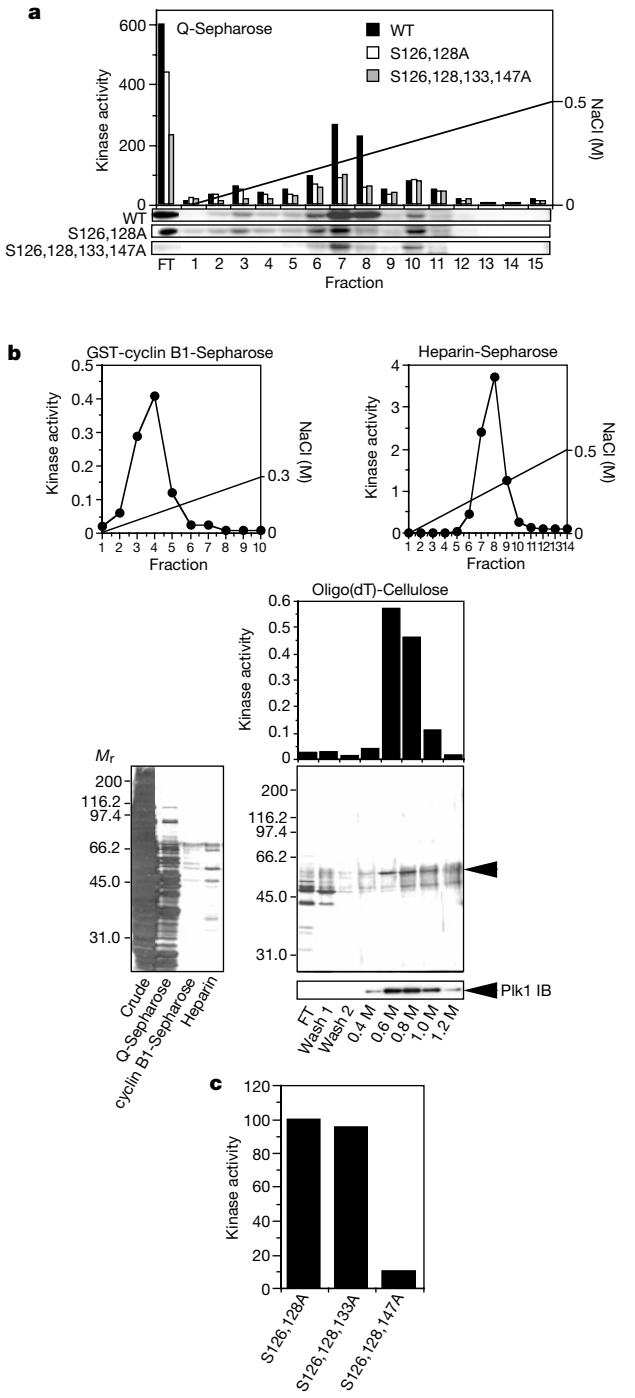

Figure 3 Purification of a kinase activity that phosphorylates S133 and/or S147 of cyclin B1. **a**, Elution profile from Q-Sepharose of the total kinase activities toward indicated substrates (top). Images of the autoradiography (bottom). **b**, Elution profiles of a kinase activity toward S126,128A-cyclin B1 (top and upper middle panels). Data are shown in arbitrary units (1 unit is 0.1 nmol min^{-1} mg^{-1}). Silver-staining of each purification step (lower middle panels) and immunoblotting with anti-Plk1 antibody (bottom panel). **c**, Kinase activitiy in the active fraction (fraction 8) of heparin–Sepharose toward the indicated forms of cyclin B1.

The 65K protein was digested with achromobacter protease I. Molecular mass analysis of the resulting Lys-C fragments determined that the 65K protein is Plx1, a *Xenopus* homologue of Plk1. Anti-Plk1 antibody reacted with the 65K protein (Fig. 3b, Oligo(dT)-Cellulose, Plk1 IB), confirming it as Plx1. This result indicates that Plx1 and Plk1 may phosphorylate S133 and/or S147 of cyclin B1 in *Xenopus* oocyte maturation and in the G2/M transition of mammalian cells, respectively.

In agreement with previous reports[24,25], both the concentration of Plk1 and the total kinase activity of Plk1 toward casein, a substrate of Plk1, increased during G2/M phase in synchronized HeLa cells (Fig. 4a, rows 5 and 6). The kinase activity of endogenous Plk1, immunoprecipitated with anti-Plk1 antibody, toward S126,128A-cyclin B1 increased in parallel with the total kinase activity of Plk1 toward casein (Fig. 4a, rows 3 and 5). This profile coincided with the kinase activity of total lysates toward S126,128A-cyclin B1 (Fig. 4a, row 1). Immunoprecipitated Plk1 barely phosphorylated S126,128,133,147A-cyclin B1 (Fig. 4a, row 4). Thus, during G2/M phase Plk1 phosphorylates cyclin B1 on S133 and/or S147 in HeLa cells.

The S126,128A-cyclin B1-phosphorylating activity in the extracts from M-phase HeLa cells was decreased to less than 10% of its original value by immunodepletion with increasing amounts of anti-Plk1 antibody, but not with control IgG (Fig. 4b, top). Bacterially produced recombinant His-tagged Plk1 protein restored the kinase activity of the Plk1-immunodepleted extract (Fig. 4b, bottom, lanes 3 and 4). These results indicate that Plk1 is a major kinase that phosphorylates S133 and/or S147 of cyclin B1 during M phase.

Recombinant His–Plk1 phosphorylated S126,128A-cyclin B1 in a dose-dependent manner, and the efficiency of the phosphorylation was almost the same as that of phosphorylating casein (Fig. 5a), indicating that cyclin B1 is a good substrate for Plk1. We next examined which of the serines S133 or S147, or both, was phosphorylated by Plk1. The active fraction of heparin–Sepharose from mature *Xenopus* oocytes (Fig. 3b) could phosphorylate S126,128A-cyclin B1 and S126,128,133A-cyclin B1, but not S126,128,147A-cyclin B1 (Fig. 3c). Recombinant His–Plk1 protein could phosphorylate S126,128A-cyclin B1 and S126,128,133A-cyclin B1, but not S133,147A-cyclin B1, S126,128,147A-cyclin B1, or S126,128,133,147A-cyclin B1 (Fig. 5b, top). Flag-tagged Plk1, purified by immunoprecipitation with anti-Flag antibody from extracts of Flag-tagged Plk1-transfected HeLa cells, also showed essentially the same substrate specificity (Fig. 5b, bottom). Moreover, recombinant His–Plk1 protein phosphorylated a synthetic peptide corresponding to residues 141–154, DLCQAFSDVILAVN, of cyclin B1 (OVA-NES), but not a phosphopeptide (DLCQAF-phosphoS^{147}-DVILAVN; OVA-P-NES) (Fig. 5c). Together, these results show that Plk1 directly phosphorylates S147 of cyclin B1.

Our results with serine/alanine mutants and serine/glutamate mutants of cyclin B1 (Fig. 1a, b) suggest that phosphorylation of S126 and S128, and of S133 and S147 cooperates to induce nuclear localization of cyclin B1. To test whether phophorylation of S147 in

Table 1 Purification of cyclin B1 kinase from *Xenopus* M-phase extracts

	Total protein (mg)	Total activity (units)	Specific activity (units per mg)	Purification (fold)
Crude extract	220			
Q-Sepharose	53	467	8.8	1.00
GST-cyclin B1-Sepharose	0.33	131	400	50.3
Heparin-Sepharose	0.050	130	2,600	292
Oligo(dT)-Cellulose	0.0015	22.8	15,200	1,710

addition to phosphorylation of the first two serines could induce nuclear localization of cyclin B1, we examined the localization of S126,128,147E-cyclin B1 and found that it localized to the nucleus (Fig. 5d). Thus, phosphorylation of the first two serines (S126 and S128) and S147 should be sufficient for nuclear translocation of cyclin B1 in prophase.

To examine whether phosphorylation of S147 of cyclin B1 occurs during prophase *in vivo*, we produced an antibody that reacts specifically with the S147-phosphorylated cyclin B1. The affinity-purified antibody (147P) recognized the synthetic phosphopeptide (OVA-P-NES), but not a non-phosphopeptide (OVA-NES) (Fig. 5e, top). It reacted with the cyclin B1 that had been immunoprecipitated with a monospecific anti-cyclin B1 antibody (Fig. 5e, middle, extract) from M-phase extracts, but it did not react with the cyclin B1 from G1/S phase (Fig. 5e, middle, anti-cyclin B1 IP). When 147P was mixed with M-phase extracts and the mixture was immunoprecipitated with the anti-cyclin B1 antibody, almost all of the 147P antibody precipitated with cyclin B1 (Fig. 5e, lower, IP; anti-cyclin B1, M). In contrast, the mixed 147P remained in the supernatant after immunoprecipitation with control IgG or when mixed with G1/S phase extracts (Fig. 5e, lower, IP; anti-cyclin B1 and IP; IgG). These data indicate that 147P recognizes specifically the S147-phosphorylated cyclin B1.

The 147P antibody immunoprecipitated cyclin B1 from synchronized HeLa cells during G2/M phase (8–10 h after release), but not from the cells in S phase (4 h after release) (Fig. 5f, bottom, IP; anti-147P) despite accumulation of significant amounts of cyclin B1 in these cells (Fig. 5f, extracts). The change in the amounts of cyclin B1 immunoprecipitated with 147P during the cell cycle matched completely the change in the kinase activity of the extracts to phosphorylate S126,128A-cyclin B1, except for a significant kinase activity in the extracts but not the immunoprecipitated cyclin B1 during late M phase, 11 h after release (Fig. 5f, S126, 128A, IP; anti-147P). This may be due to degradation of endogenous cyclin B1 in late M phase (Fig. 5f, bottom).

Immunohistochemistry of HeLa cells with 147P (Fig. 5g) showed that metaphase cells (white arrowheads), but not S-G2 phase (red

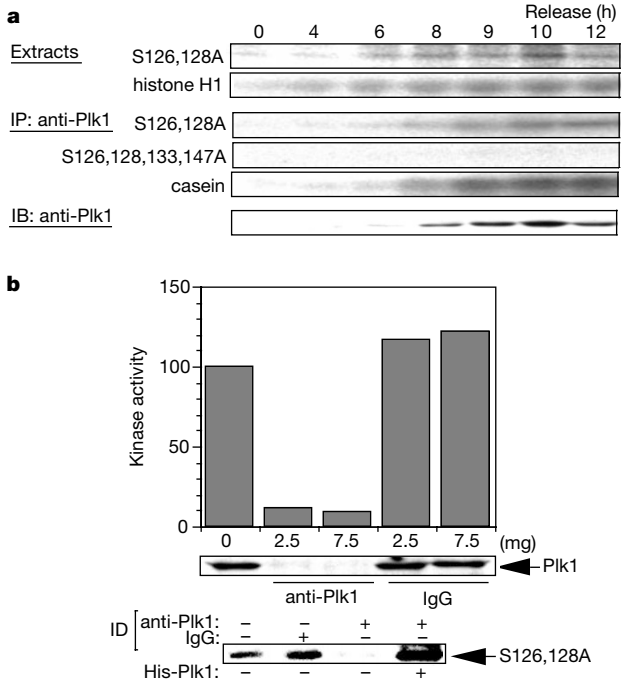

Figure 4 Plk1 phosphorylates cyclin B1 on S133 and/or S147 during G2/M phase in HeLa cells. **a**, Kinase activities in the extracts and that of endogenous Plk1 (IP; anti-Plk1). The extracts were immunoblotted with anti-Plk1 antibody (IB; anti-Plk1). **b**, Immunodepletion (ID) of M-phase extracts with increasing amounts of anti-Plk1 antibody or non-immunized rabbit IgG. Kinase activity toward GST–S126,128A-cyclin B1 remaining in the supernatant (top) and the immunoblotting with anti-Plk1 antibody (middle) are shown. His-tagged Plk1 (0.1 μg) was added to the Plk1-depleted M-phase extracts (bottom). Kinase activities toward GST–S126,128A-cyclin B1 are shown.

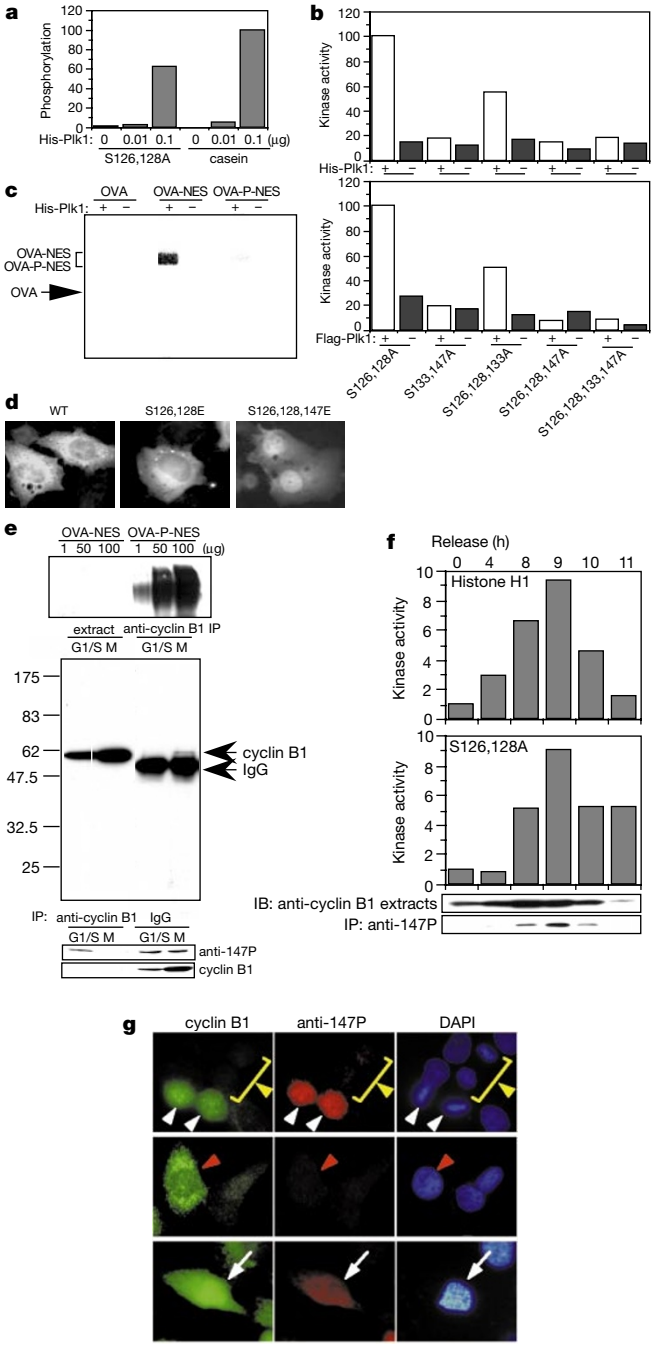

Figure 5 Plk1-mediated phosphorylation of cyclin B1 on S147 *in vitro* and *in vivo*. **a**, Phosphorylation of GST–S126,128A-cyclin B1 and casein (20 pmol of each) by His–Plk1. **b**, Kinase activities of His–Plk1 (0.01 μg) (top) and Flag–Plk1 toward the indicated forms of cyclin B1 (1 μg). **c**, Kinase activities of His–Plk1 (1 μg) toward OVA, OVA-NES and OVA-P-NES (0.2 μg each). Similar results were obtained using 0.1 μg His-tagged Plk1 and 0.02 μg of substrates. **d**, Subcellular localization of HA-tagged WT cyclin B1, HA–S126,128E-cyclin B1 and HA–S126,128,147E-cyclin B1. **e**, Specificity of anti-147P (see Methods). **f**, Kinase activities in the extracts toward histone H1 and S126,128-cyclin B1 (top and bottom graphs). Extracts and the immunoprecipitates with anti-147P were immunoblotted with anti-cyclin B1 antibody (bottom panels). **g**, HeLa cells were stained with anti-cyclin B1 antibody (left), anti-147P (middle) or DAPI (right).

arrowhead), anaphase (not shown), telophase (yellow arrowhead) or G1 phase cells (not shown), were stained with this antibody. This antibody stained also prophase cells (white arrow). These results show that phosphorylation of S147 of cyclin B1 occurs during G2/M phase *in vivo*.

Our results indicate that Plk1 phosphorylation of cyclin B1 on S147 during prophase is central to inducing nuclear translocation of cyclin B1. As S126 and S128 of cyclin B1 are reported to be phosphorylated by Cdc2 (refs 14, 21, 23), activation of Plk1 should induce nuclear translocation of S126,128E-cyclin B1. To test this, we co-expressed Plk1 and S126,128E-cyclin B1 in HeLa cells. Experiments were performed in the presence of MG132, a proteasome inhibitor, to avoid degradation of cyclin B1, as Plk1 phosphorylates and activates the anaphase-promoting complex (APC), facilitating degradation of cyclin B1. Treatment with MG132 alone had no effect on the subcellular localization of cyclin B1 (data not shown). When co-expressed with wild-type Plk1, the S126,128E-cyclin B1 remained in the cytoplasm (Fig. 6a, WT). We next co-transfected a constitutively active Plk1 (SDTD-Plk1), constructed by a published method[26], and found that the S126,128E-cyclin B1 accumulated strongly in the nucleus (Fig. 6a, SDTD).

To exclude possible involvement of the kinase activity of Cdc2, we carried out experiments in the presence of butyrolactone I, a specific CDK inhibitor, at a concentration enough to induce cell-cycle arrest at G2 phase but not apoptosis in HeLa cells. S126,128E-cyclin B1 still accumulated strongly in the nucleus when SDTD-Plk1 was co-expressed (Fig. 6a, SDTD+butyrolactone I), indicating that activation of Plk1 can induce nuclear entry of S126,128E-cyclin B1 in the absence of Cdc2 activity. Because expression of SDTD-Plk1 did not induce nuclear translocation of MAP kinase kinase MEK1 (data not shown), whose cytoplasmic localization is maintained by its nuclear export signal (NES), we could exclude the possibility that Plk1 may inhibit the nuclear export system.

To further investigate the role of phosphorylation of cyclin B1 in its nuclear localization, we co-expressed various forms of cyclin B1 with SDTD-Plk1. In most transfected cells (~70–80%), both S126,128,133,147A-cyclin B1 and S133,147A-cyclin B1 remained in the cytoplasm even in the presence of SDTD-Plk1 (Fig. 6b, S126, 128, 133, 147A and S133,147A). This result supports our idea that Plk1 phosphorylates S147 and induces nuclear localization of cyclin B1. In contrast, in more than half of the transfected cells, both wild-type and S126,128A-cyclin B1, localized in the nucleus (Fig. 6b, WT and S126,128A). Thus, the phosphorylation of S126 and/or S128, which is catalysed by Cdc2, may not be absolutely required for the Plk1-induced nuclear localization of cyclin B1. As nuclear localization of wild-type and S126,128A-cyclin B1 was less complete than that of S126,128E-cyclin B1 (Fig. 6b), however, phosphorylation of S126 and/or S128 may also contribute to stimulation of the nuclear localization of cyclin B1.

We have identified Plk1 as a protein kinase that phosphorylates a serine residue (S147) in the NES of cyclin B1 and targets it to the nucleus during prophase in vertebrate cells. The Plk1-mediated phosphorylation seems to be responsible for inactivating the NES of cyclin B1 rather than enhancing nuclear import of cyclin B1, because we observed that OVA-P-NES, when injected into the nucleus, was exported from the nucleus to the cytoplasm more slowly than OVA-NES, and that OVA-P-NES, when injected into the cytoplasm, did not move into the nucleus (data not shown). It is possible, however, that phosphorylation of several serines including S147 may create a nuclear import signal and enhance the nuclear import of cyclin B1 (ref. 14).

During G2/M phase, Cdc2 is activated and Plk1 is synthesized and activated. Thus, the activation of the kinase activity of MPF (Cdc2–cyclin B1 complex) and its nuclear translocation may occur coordinately. Previous work has suggested that Plk1 might activate Cdc2 by phosphorylating and activating Cdc25C (refs 16, 27), and that a positive feedback loop might exist between Plk1 and MPF. We speculate that Plk1 may coordinate the activation of MPF and its nuclear translocation. □

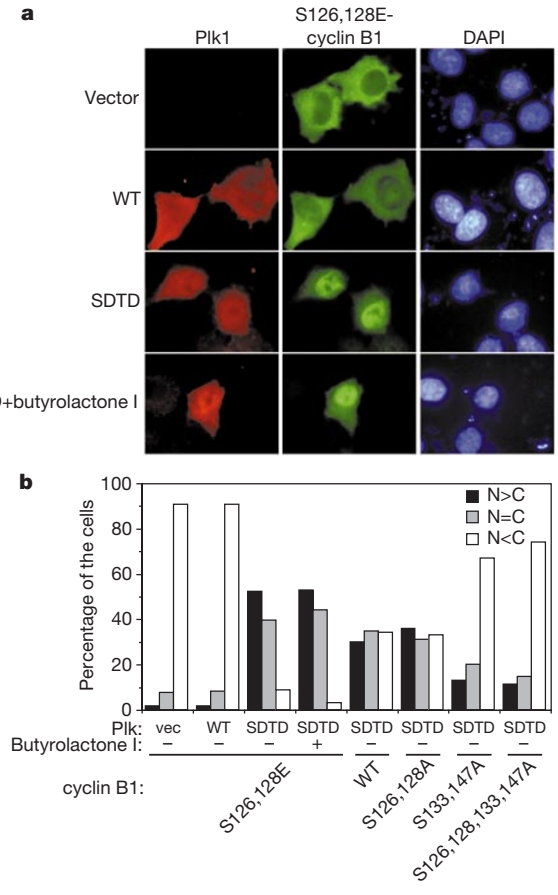

Figure 6 Constitutively active Plk1 induces nuclear localization of cyclin B1 in the absence of Cdc2 kinase activity. **a**, HeLa cells were co-transfected with a plasmid containing Myc–S126,128E-cyclin B1 and control vector, HA-tagged wild-type Plk1 or HA–SDTD-Plk1. After 15 h, cells were incubated with MG132 (50 μM) in the absence or presence of butyrolactone I (120 μM) for 6 h and then immunostained with anti-Myc and anti-HA antibodies. **b**, Cells were classified into three categories in terms of location of Myc–cyclin B1 as described in the legend of Fig. 1b. More than 200 cells were examined, and the percentages of each categories are shown. Experiments were performed twice with similar results.

Methods

Protein preparation

GST–cyclin B1 and His-tagged Plk1 were prepared as described[10]. His-tagged Plk1 was further purified by Mono-Q with a linear gradient to 1 M NaCl, and the active fractions were used for *in vitro* kinase assays.

Immunoprecipitation, immunoblotting and cell staining

Cells were lysed in buffer 1 (20 mM HEPES pH 7.4, 20 mM 2-glycerophosphate, 2 mM EGTA, 1.5 mM $MgCl_2$, 150 mM NaCl, 50 mM NaF, 0.5% NP-40, 2 mM dithiothreitol (DTT), 1 mM Na_3VO_4, 1 mM PMSF, 2 μg ml^{-1} aprotinin, 1 μM okadaic acid) containing 10% glycerol, and centrifuged at 20,000*g* for 15 min. Endogenous Plk1 or Flag-tagged Plk1 was immunoprecipitated with anti-Plk1 (Zymed) or anti-Flag antibody (Sigma). Immunoblotting and immunofluorescent cell staining were done as described[10,28].

Kinase assays

We lysed cells in buffer 2 (20 mM Tris pH 7.5, 60 mM 2-glycerophosphate, 10 mM EGTA, 10 mM $MgCl_2$, 10 mM NaF, 0.1% NP-40, 1 mM DTT, 1 mM Na_3VO_4, 1 mM PMSF, 2 μg ml^{-1} aprotinin, 1 μM okadaic acid), and centrifuged them at 20,000*g* for 15 min. The supernatant was mixed with 1 μg of substrate, 100 μM ATP, 15 mM $MgCl_2$, 2 μCi of [γ^{32}-P]ATP and incubated for 40 min at 25 °C. Histone H1 kinase assay was done as described[10]. In the kinase assays for His-tagged Plk1 or immunoprecipitates, 0.01 μg,

0.1 μg or 1 μg of His-tagged Plk1 or immunoprecipitates was mixed with substrates (casein or GST–cyclin B1, 0.1–1 μg), 50 μM ATP, 15 mM $MgCl_2$, 3 μCi of [γ^{32}-P]ATP and incubated for 20 min at 30 °C.

Purification of cyclin B1 kinase

De-jellied *Xenopus* eggs (50 ml) were homogenized in four volumes of buffer A (50 mM Tris pH 8.0, 25 mM 2-glycerophosphate, 10 mM EGTA, 10 mM $MgCl_2$, 0.1 mM NaF, 2 mM DTT, 1 mM Na_3VO_4, 2 mM PMSF) with 10 μg ml^{-1} cytochalasin B and 20 μg ml^{-1} aprotinin, centrifuged at 20,000*g* for 30 min and then 140,000*g* for 1 h, and was loaded onto a 50-ml Q-Sepharose Fast Flow (Pharmacia). Unadsorbed fractions were loaded onto a cyclin B1 affinity column, GST–S126,128,133,147A-cyclin B1 coupled to glutathione–Sepharose, equilibrated with buffer B (20 mM Tris pH 7.3, 12.5 mM 2-glycerophosphate, 2 mM EGTA, 2 mM $MgCl_2$, 2 mM DTT, 1 mM Na_3VO_4, 1 mM PMSF, 2 μg ml^{-1} aprotinin). Proteins were eluted with a linear gradient to 1 M NaCl and assayed for the kinase activity toward GST–S126,128A-cyclin B1. Active fractions were loaded onto Hitrap–Heparin (Pharmacia), and eluted with a linear gradient to 1 M NaCl in buffer B. The active fractions were adjusted to 0.25 M NaCl, loaded onto oligo(dT)-cellulose (GibcoBRL) equilibrated with buffer B containing 0.25 M NaCl, and eluted stepwise with buffer B containing 0.4, 0.6, 0.8, 1.0 and 1.2 M NaCl.

Identification of proteins by peptide mass mapping

Samples were electrophoresed on a 9% polyacrylamide gel and transferred onto a PDVF membrane. The immobilized proteins were reduced, S-carboxymethylated, and digested *in situ* with Achromobactor protease I (a Lys-C)[29]. Molecular mass analysis of Lys-C fragments was performed by spectrometry using a PerSeptive Biosystem Voyager-DE/RP[30]. We identified proteins by comparing the molecular weights determined by MALDI-TOF/MS with theoretical peptide masses from the proteins registered in NCBInr (10 April 1999).

Anti-S147-phosphorylated cyclin B1 antibody (147P)

Anti-S147-phosphorylated cyclin B1 polyclonal antibody was produced in rabbits by immunizing them with a keyhole limpet haemocyanin-conjugated synthetic phosphopeptide corresponding to residues 141–154 of cyclin B1 (DLCQAF-phosphoS147-DVILAVN). The serum was affinity purified with the phosphopeptide- and the non-phosphopeptide (DLCQAFDVILAVN)-conjugated cellulose. The purified 147P antibody was added to the cell extracts and the immunoprecipitates were washed three times and immunoblotted with anti-cyclin B1. In the immunoprecipitation with 147P from the immunoprecipitates with anti-cyclin B1, endogenous cyclin B1 was first immunoprecipitated with anti-cyclin B1, washed three times, and then released from the beads by incubating in the presence of 1% SDS. After the beads were discarded, supernatants were diluted 10 times and then immunoprecipitated with anti-147P. In the assay shown in Fig. 5e, bottom panel, anti-147P and agarose-conjugated anti-cyclin B1 or IgG were added to the extracts. Supernatants were immunoblotted with horseradish peroxidase-conjugated anti-rabbit immunoglobulins (Amersham) and anti-cyclin B1 to detect anti-147P and cyclin B1, respectively.

Received 31 October; accepted 15 December 2000.

1. Nurse, P. Universal control mechanism regulating onset of M-phase. *Nature* **344,** 503–508 (1990).
2. Hunt, T. Cyclins and their partners: from a simple idea to complicated reality. *Semin. Cell Biol.* **2,** 213–222 (1991).
3. Morgan, D. O. Principles of CDK regulation. *Nature* **374,** 131–134 (1995).
4. Pines, J. & Hunter, T. Human cyclins A and B1 are differentially located in the cell and undergo cell cycle-dependent nuclear transport. *J. Cell Biol.* **115,** 1–17 (1991).
5. Ookata, K., Hisanaga, S., Okano, T., Tachibana, K. & Kishimoto, T. Relocation and distinct subcellular localization of p34cdc2–cyclin B complex at meiosis reinitiation in starfish oocytes. *EMBO J.* **11,** 1763–1772 (1992).
6. Pines, J. & Hunter, T. The differential localization of human cyclins A and B is due to a cytoplasmic retention signal in cyclin B. *EMBO J.* **13,** 3772–3781 (1994).
7. Heald, R., McLoughlin, M. & McKeon, F. Human wee1 maintains mitotic timing by protecting the nucleus from cytoplasmically activated Cdc2 kinase. *Cell* **74,** 463–474 (1993).
8. Li, J., Meyer, A. N. & Donoghue, D. J. Nuclear localization of cyclin B1 mediates its biological activity and is regulated by phosphorylation. *Proc. Natl Acad. Sci. USA* **94,** 502–507 (1997).
9. Jin, P., Hardy, S. & Morgan, D. O. Nuclear localization of cyclin B1 controls mitotic entry after DNA damage. *J. Cell Biol.* **141,** 875–885 (1998).
10. Toyoshima, F., Moriguchi, T., Wada, A., Fukuda, M. & Nishida, E. Nuclear export of cyclin B1 and its possible role in the DNA damage-induced G2 checkpoint. *EMBO J.* **17,** 2728–2735 (1998).
11. Yang, J. & Kornbluth, S. All aboard the cyclin train: subcellular trafficking of cyclins and their CDK partners. *Trends Cell Biol.* **9,** 207–210 (1999).
12. Pines, J. Four-dimensional control of the cell cycle. *Nature Cell Biol.* **1,** E73–E79 (1999).
13. Yang, J. *et al.* Control of cyclin B1 localization through regulated binding of the nuclear export factor CRM1. *Genes Dev.* **12,** 2131–2143 (1998).
14. Hagting, A., Jackman, M., Simpson, K. & Pines, J. Translocation of cyclin B1 to the nucleus at prophase requires a phosphorylation-dependent nuclear import signal. *Curr. Biol.* **9,** 680–689 (1999).
15. Hagting, A., Karlsson, C., Clute, P., Jackman, M. & Pines, J. MPF localization is controlled by nuclear export. *EMBO J.* **17,** 4127–4138 (1998).
16. Kumagai, A. & Dunphy, W. G. Purification and molecular cloning of Plx1, a Cdc25-regulatory kinase from *Xenopus* egg extracts. *Science* **273,** 1377–1380 (1996).
17. Glover, D. M., Hagan, I. M. & Tavares, A. A. Polo-like kinases: a team that plays throughout mitosis. *Genes Dev.* **12,** 3777–3787 (1998).
18. Nigg, E. A. Polo-like kinases: positive regulators of cell division from start to finish. *Curr. Opin. Cell Biol.* **10,** 776–783 (1998).
19. Jackman, M., Firth, M. & Pines, J. Human cyclins B1 and B2 are localized to strikingly different structures: B1 to microtubules, B2 primarily to the Golgi apparatus. *EMBO J.* **14,** 1646–1654 (1995).
20. Nigg, E. A. Assembly–disassembly of the nuclear lamina. *Curr. Opin. Cell Biol.* **4,** 105–109 (1992).
21. Izumi, T. & Maller, J. L. Phosphorylation of *Xenopus* cyclins B1 and B2 is not required for cell cycle transitions. *Mol. Cell. Biol.* **11,** 3860–3867 (1991).
22. Li, J., Meyer, A. N. & Donoghue, D. J. Requirement for phosphorylation of cyclin B1 for *Xenopus* oocyte maturation. *Mol. Biol. Cell* **6,** 1111–1124 (1995).
23. Borgne, A., Ostvold, A. C., Flament, S. & Meijer, L. Intra-M phase-promoting factor phosphorylation of cyclin B at the prophase/metaphase transition. *J. Biol. Chem.* **274,** 11977–11986 (1999).
24. Golsteyn, R. M., Mundt, K. E., Fry, A. M. & Nigg, E. A. Cell cycle regulation of the activity and subcellular localization of Plk1, a human protein kinase implicated in mitotic spindle function. *J. Cell Biol.* **129,** 1617–1628 (1995).
25. Hamanaka, R. *et al.* Polo-like kinase is a cell cycle-regulated kinase activated during mitosis. *J. Biol. Chem.* **270,** 21086–21091 (1995).
26. Qian, Y. W., Erikson, E. & Maller, J. L. Mitotic effects of a constitutively active mutant of the *Xenopus* Polo-like kinase Plx1. *Mol. Cell. Biol.* **19,** 8625–8632 (1999).
27. Qian, Y. W., Erikson, E., Li, C. & Maller, J. L. Activated polo-like kinase Plx1 is required at multiple points during mitosis in *Xenopus laevis*. *Mol. Cell. Biol.* **18,** 4262–4271 (1998).
28. Fukuda, M. *et al.* CRM1 is responsible for intracellular transport mediated by the nuclear export signal. *Nature* **390,** 308–311 (1997).
29. Iwamatsu, A. S-carboxymethylation of proteins transferred onto polyvinylidene difluoride membranes followed by *in situ* protease digestion and amino acid microsequencing. *Electrophoresis* **13,** 142–147 (1992).
30. Jensen, O. N., Podtelejnikov, A. & Mann, M. Delayed extraction improves specificity in database searches by matrix-assisted laser desorption/ionization peptide maps. *Rapid Commun. Mass Spectrom.* **10,** 1371–1378 (1996).

Acknowledgements

We are grateful to K. Todokoro for a mouse Plk1 complementary DNA and to H. Ellinger-Ziegelbauer for advice on Plk1 assays. We thank M. Yanagida for helpful discussion. This work was supported by grants from the Ministry of Education, Science and Culture of Japan (E.N.).

Correspondence and requests for materials should be addressed to E.N. (e-mail: L50174@sakura.kudpc.kyoto-u.ac.jp).

The *S*-locus receptor kinase is inhibited by thioredoxins and activated by pollen coat proteins

Didier Cabrillac, J. Mark Cock, Christian Dumas & Thierry Gaude

Reproduction et Développement des Plantes, UMR 5667 CNRS-INRA-ENSL-UCBL Ecole Normale Supérieure de Lyon, 46 Allée d'Italie, 69364 Lyon Cedex 07, France

The self-incompatibility response in *Brassica* allows recognition and rejection of self-pollen by the stigmatic papillae. The transmembrane *S*-locus receptor kinase (SRK), a member of the receptor-like kinase superfamily in plants, mediates recognition of self-pollen on the female side[1], whereas the *S*-locus cysteine-rich protein (SCR) is the male component of the self-incompatibility response[2]. SCR is presumably located in the pollen coat, and is thought to be the SRK ligand[2,3]. Although many receptor-like kinases have been isolated in plants, the mechanisms of signal transduction mediated by these molecules remain largely unknown. Here we show that SRK is phosphorylated *in vivo* within one hour of self-pollination. We also show that, *in vitro*, autophosphorylation of SRK is prevented by the stigma thioredoxin THL1 in the absence of a ligand. This inhibition is released in a haplotype-specific manner by the addition of pollen coat proteins. Our data indicate that SRK is inhibited by thioredoxins and activated by pollen coat proteins.

To investigate the phosphorylation status of SRK during the self-incompatibility reaction, we labelled pistils from self-incompatible S_3 homozygous *Brassica oleracea* plants with [^{32}P]orthophosphate, and monitored phosphorylation of the receptor during a self-pollination time course. Physiological studies have shown that